Molecular Therapy
Original Article

Corneal fibrosis abrogation by a localized AAV-mediated *inhibitor of differentiation 3* (*Id3*) gene therapy in rabbit eyes *in vivo*

Suneel Gupta,[1,2,6] Michael K. Fink,[3,6] Duraisamy Kempuraj,[1,2] Nishant R. Sinha,[1,2] Lynn M. Martin,[1,2] Landon M. Keele,[1,2] Prashant R. Sinha,[1,2] Elizabeth A. Giuliano,[1,2] Nathan P. Hesemann,[1,3] Sudhanshu P. Raikwar,[1,2] Shyam S. Chaurasia,[1,2,5] and Rajiv R. Mohan[1,2,4]

[1]Harry S. Truman Memorial Veterans' Hospital, Columbia, MO 65201, USA; [2]Departments of Veterinary Medicine & Surgery and Biomedical Sciences, College of Veterinary Medicine, University of Missouri, 1600 East Rollins Street, Columbia, MO 65211, USA; [3]Department of Pathology, School of Medicine, University of Colorado Denver Anschutz Medical Campus, Aurora, CO 80045, USA; [4]Mason Eye Institute, School of Medicine, University of Missouri, 1600 East Rollins Street, Columbia, MO 65212, USA; [5]Department of Ophthalmology & Visual Sciences, Medical College of Wisconsin, Milwaukee, WI 53226, USA

Previously we found that *inhibitor of differentiation 3* (*Id3*) gene, a transcriptional repressor, efficiently inhibits corneal keratocyte differentiation to myofibroblasts *in vitro*. This study evaluated the potential of adeno-associated virus 5 (AAV5)-mediated *Id3* gene therapy to treat corneal scarring using an established rabbit *in vivo* disease model. Corneal scarring/fibrosis in rabbit eyes was induced by alkali trauma, and 24 h thereafter corneas were administered with either balanced salt solution AAV5-naked vector, or AAV5-Id3 vector (n = 6/group) via an optimized reported method. Therapeutic effects of AAV5-Id3 gene therapy on corneal pathology and ocular health were evaluated with clinical, histological, and molecular techniques. Localized AAV5-Id3 gene therapy significantly inhibited corneal fibrosis/haze clinically from 2.7 to 0.7 on the Fantes scale in live animals (AAV5-naked versus AAV5-Id3; $p < 0.001$). Furthermore, AAV5-Id3 treatment significantly reduced profibrotic gene mRNA levels: α-smooth muscle actin (α-SMA) (2.8-fold; $p < 0.001$), fibronectin (3.2-fold; $p < 0.001$), collagen I (0.8-fold; $p < 0.001$), and collagen III (1.4-fold; $p < 0.001$), as well as protein levels of α-SMA (23.8%; $p < 0.001$) and collagens (1.8-fold; $p < 0.001$). The anti-fibrotic activity of AAV5-Id3 is attributed to reduced myofibroblast formation by disrupting the binding of E-box proteins to the promoter of α-SMA, a transforming growth factor-β signaling downstream target gene. In conclusion, these results indicate that localized AAV5-Id3 delivery in stroma caused no clinically relevant ocular symptoms or corneal cellular toxicity in the rabbit eyes.

INTRODUCTION

Corneal blindness is a global leading cause of blindness. About 10 million people have bilateral corneal blindness, 39 million people have no vision, and more than 246 million people have moderate/severe vision impairment worldwide.[1–3] Eye trauma and corneal ulcer are among the top insults and are linked to causing 1.5–2 million new cases of corneal blindness each year.[4] Corneal disorders instigate vision loss in roughly 4% of the United States population. According to the National Eye Institute, the annual economic burden of ocular disorders including blindness in America alone is $139 billion.[2,5] At present, there are limited treatment modalities available for effectively treating corneal scarring in patients. In terms of topical treatment modalities, the current pharmaceutical options still rely on intraoperative drugs and steroids such as mitomycin C (MMC) for the prevention of corneal haze.[4–8] These treatments can have numerous adverse effects, and there is a debate among clinicians about the correct dosing and duration of use for such medications as safe treatments for corneal scarring.[9–11] Recently, limbal stem cell therapy appeared as a promising treatment choice. However, the success of stem cell therapies relies on the availability of donor ocular tissues in addition to considerations of maintenance, transportation, cell-culturing techniques, long-term storage, and expansion. These are the major hurdles to the viability of limbal stem cell therapy as a readily available treatment option.[12–14] Current topical therapies for corneal haze or scarring provide only short-term relief, require multiple applications, cause a variety of side effects, and often fail. Currently, donor cornea transplant surgery is a standard of care to restore corneal function and vision. However, 53% of the world's population have no access to donor corneas for surgical intervention and 12.7 million people around the world are waiting for corneal transplantation.[1] The successful use of donor corneal tissues always depends on the screening parameters, preservation techniques, storage, transport, and the detailed clinical evaluation of the donor corneas, which are the major hurdles of this process. Furthermore, the supply of transplantable

Received 16 February 2022; accepted 29 June 2022;
https://doi.org/10.1016/j.ymthe.2022.06.018.

[6]These authors contributed equally

Correspondence: Rajiv R. Mohan, PhD, FARVO, Professor of Ophthalmology and Molecular Medicine, University of Missouri, 1600 East Rollins Street, Columbia, MO 65211, USA.
E-mail: mohanr@health.missouri.edu

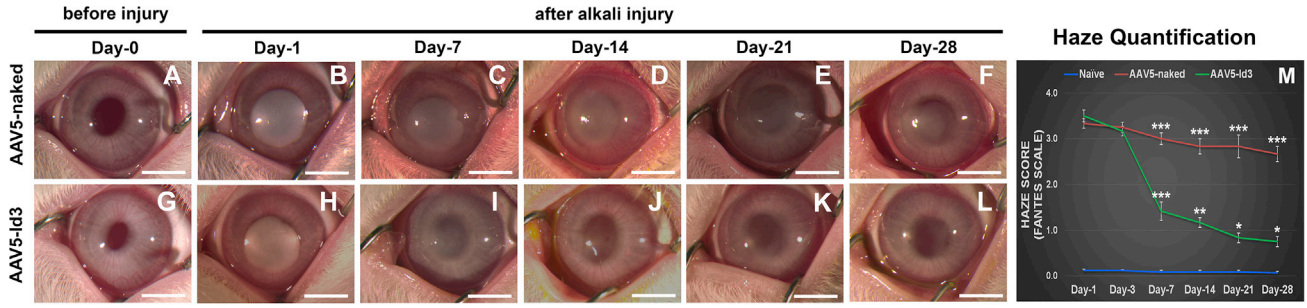

Figure 1. AAV5-Id3 gene therapy regulates corneal fibrosis and maintains corneal transparency

(A–F) Stereo-biomicroscopic images show the progress of alkali trauma in the AAV5-naked vector group in a time-dependent manner. (G–L) Stereo-biomicroscopic images show the progress and efficacy of AAV5-Id3 gene therapy after alkali trauma in the AAV5-Id3 group in a time-dependent manner. (M) Haze quantification graph on the Fantes scale shows the impact of AAV5-Id3 gene therapy in corneal tissue. There were six samples in each group, and error bars represent ±SEM. *$p < 0.05$; **$p < 0.01$; ***$p < 0.001$. Scale bars, 3.0 mm.

donor corneas is depleting because of HIV infection and refractive laser surgeries such as PRK, LASIK, and LASEK in the United States and other developed countries. Therefore, the development of non-surgical efficacious and safe modalities for corneal scarring and other prevalent corneal disorders is important.

Corneal transplantation remains the most feasible choice for the successful treatment of corneal scarring through surgical intervention.[15–17] However, high cost along with the limited supply of good donor corneas, potential surgical complications, and graft rejections restrict the widespread use of surgical intervention for corneal disorders.[18]

The etiology and underlying molecular mechanism of corneal scarring have been explored over the last several decades. Keratocyte migration, proliferation, and differentiation play a dominant role in corneal wound healing, remodeling, and transparency resurgence. Under traumatic stress, disruption of the homeostatic balance of cytokines, chemokines, growth factors, and transcription factors leads to pathological conditions in the cornea such as scarring and impaired vision.[1–3] The decisive role of transforming growth factor β (TGF-β), suppressor of mothers against decapentaplegic signaling (Smad), and bone morphogenetic proteins (BMPs) in fibrotic signaling regulating keratocyte differentiation is documented in the literature.[19–21] These upstream regulators govern cell-cycle arrest, inhibit cellular proliferation, and promote differentiation or apoptosis by targeting numerous transcription factors, which include runt-related transcription factor 1 (RUNX1), basic-helix-loop-helix (bHLH), forkhead transcription factor, specificity protein 1, activator protein 1, and inhibitor of differentiation (Id) genes.[22–24] The bHLH proteins and *Id*s play an essential role in directing cell fate by regulating the transcription of various genes. Id proteins are a subfamily of regulatory dimeric bHLH transcription factors that bind to E-box (CANNTG) sequences on the promoter region of target gene factors to regulate cellular events such as cell growth, proliferation, and differentiation.[25–27] Earlier, we characterized all four *Id*s in the human cornea and reported their role in differentiation cascades through targeting of TGF-β/Smad signaling via bHLH protein and E-box sequences using an established *in vitro* corneal fibrosis model.[23,24]

Our previous work suggested that TGF-β/Smad hyperactivity synchronizes the differentiation cascades and that the HLH protein Id3 controls the transcription machinery of the differentiation process by modulating the heterodimer with E-box protein in corneal wound healing.[23,24] The findings of our *in vitro* research led to a novel postulate that the *Id3* gene delivered into corneal stroma in a tissue-targeted manner with an AAV5 vector via a reported topical technique can offer an effective gene therapy method to treat corneal fibrosis *in vivo*. This study tested the therapeutic potential, safety, and tolerability of AAV5-Id3 gene therapy in preventing excessive wound-healing process and as a successful treatment modality for corneal scarring using an established preclinical rabbit *in vivo* model.

RESULTS

Clinical-level evaluation of AAV5-Id3 on corneal fibrosis and transparency

AAV5-Id3 gene therapy delivered 24 h post alkali trauma into corneal stroma significantly attenuated existing corneal fibrosis and restored corneal transparency *in vivo* (Figures 1A–1L). The central corneas of all rabbits were transparent before alkali injury (Figures 1A and 1G) and subsequently developed severe opacification within 1 day of alkali injury (Figures 1B and 2H). AAV5-Id3 or AAV5-naked vector was topically administered into stroma 24 h after alkali injury. Rabbit corneas receiving *Id3* gene therapy (AAV5-Id3) demonstrated clinically significant amelioration of corneal fibrosis/opacification and a concurrent time-dependent increase in corneal transparency on day 7 (Figure 1I), day 14 (Figure 1J), day 21 Figure 1K), and day 28 (Figure 1L) compared with the corneas that received no gene therapy (AAV5-naked) (Figures 1C–1F). In addition, the rabbit eyes that received *Id3* gene therapy showed marked reductions in clinical corneal edema, ocular inflammation, scleral hyperemia, and ocular discharge after day 14. Quantitative clinical corneal haze scores on Fantes grading were evaluated by at least two masked observers

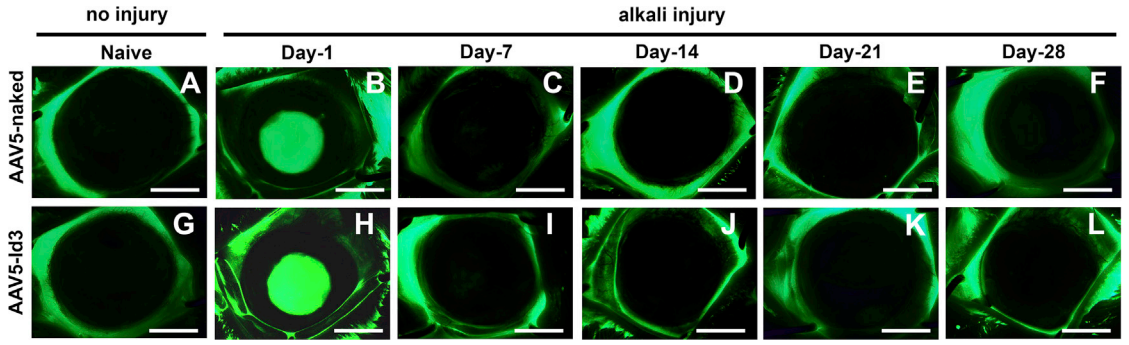

Figure 2. AAV5-Id3 gene therapy does not impact corneal re-epithelialization

(A–L) Fluorescein eye test microscopic images show that the re-epithelialization patterns were the same in the AAV5-naked vector and AAV5-Id3 gene-delivered groups of animal corneal tissue in a time-dependent manner. (B) and (H) show that corneal epithelium was not a present post-alkali injury at day 1 in AAV5-naked vector and AAV5-Id3 gene-delivered groups. (C) and (I) show the regular turnover of the corneal epithelium post alkali injury at day 7 in AAV5-naked vector and AAV5-Id3 gene-delivered groups. Scale bars, 3.0 mm.

(Figure 1M). The AAV5-Id3 gene therapy produced a statistically significant reduction in corneal haze at day 7 (2.1-fold; $p < 0.001$), day 14 (2.5-fold; $p < 0.001$), day 21 (3.4-fold; $p < 0.001$), and day 28 (3.5-fold; $p < 0.001$) compared with the corresponding AAV5-naked delivered corneas. No significant differences in haze scores were noted in the AAV5-Id3 and AAV5-naked groups on day 1 and day 3. The slit-lamp-based subjective clinical evaluations (Figure S1) concurred with the stereo biomicroscopy evaluations and the respective Fantes haze scores shown in Figure 1. AAV5-Id3 gene delivery led to clinical resolution of corneal fibrosis but did not adversely affect typical physiological wound healing (Figures S1A–S1L). Representative slit-lamp images showed no evidence of corneal haze at baseline (Figures S1A and S1G) and a dense haze on day 1 post injury (Figures S1B and S1H). A significant decrease in the haze was detected from day 7 onward until day 28 in AAV5-Id3-delivered corneas (Figures S1I–S1L) compared with AAV5-naked corneas (Figures S1C–S1F). On day 28, corneal haze scores were 0.7 versus 2.6 ($p < 0.001$) in the AAV5-Id3 and AAV5-naked groups, respectively.

Fluorescein staining showed that AAV5-Id3 gene therapy is not deleterious to corneal re-epithelialization (Figure 2). Fluorescent biomicroscopic images displayed normal epithelium at baseline (Figures 2A and 2G) and a focal loss of epithelium in the central cornea 1 day after alkali injury (Figures 2B and 2H), and complete re-epithelialization and negative fluorescein staining by day 7 (Figures 2C and 2I). Overall, AAV5-Id3 gene therapy did not impact corneal re-epithelialization compared with the AAV5-naked or balanced salt solution (BSS)-treated animal groups.

Optical coherence tomography (OCT) images of rabbit corneas collected 28 days post alkali injury exhibited pathologic changes including increased epithelial reflectivity, focal regions of hyperintensity within the stroma, and increased corneal thickness compared with naive corneas (Figure 3). The sequelae to corneal injury were markedly attenuated in the AAV5-Id3 group compared with the AAV5-naked group (Figures 3B and 3C).

The mid-stromal region (central corneal injury zone) on confocal biomicroscopy showed a prominent arrangement of the basal nerve plexus in the naive control group (Figure 3D). In the AAV5-naked group the keratocyte population was not visible, while in the AAV5-Id3 group the keratocyte population and nerve plexus were organized in an improved manner (Figure 3F) compared with the AAV5-naked group at day 28. The gross OCT analysis found the keratocyte population and stromal reorganization to be close to naive controls in AAV5-Id3-treated corneas. At the same time, the mid-stromal region (peripheral non-injury zone) showed no prominent difference in the arrangement of the nucleus, basal nerve plexus, and keratocyte organization pattern in naive, AAV5-naked, and AAV5-Id3-treated groups (Figures 3G–3I).

Effect of AAV5-Id3 gene therapy on corneal fibrosis

AAV5-Id3 gene therapy to rabbit corneas post alkali trauma resulted in improved wound healing. The fibrotic markers, mRNA, and protein levels supported the clinical observations seen in live animals. The quantitative real-time PCR (qRT-PCR) mRNA expression of four profibrotic marker genes (α-smooth muscle actin [α-SMA], fibronectin, collagen I, and collagen III) were evaluated in the corneas of naive, AAV5-naked, and AAV5-Id3 groups post euthanasia at day 28 (Figures 4A–4D). Alkali trauma significantly elevated the expression of four tested profibrotic genes in the AAV5-naked corneas compared with the naive corneas (5.38 ± 0.34-fold; $p < 0.001$), while AAV5-Id3 gene transfer significantly reduced expression of α-SMA (2.08 ± 0.47-fold; $p < 0.001$), fibronectin (3.11 ± 0.29-fold; $p < 0.001$), collagen I (1.69 ± 0.33-fold; $p < 0.001$), and collagen III (2.07 ± 0.41-fold; $p < 0.001$) compared with the non-therapy corneas (AAV5-naked).

Histological analysis further revealed that AAV5-Id3 gene therapy had a profound inhibitory effect on myofibroblast formation (Figures 4E–4H) and collagen levels (Figures 4I–4L). Immunofluorescence analysis of a myofibroblast marker, α-SMA, found significantly reduced α-SMA-positive cells in AAV5-Id3 corneas (Figure 4F)

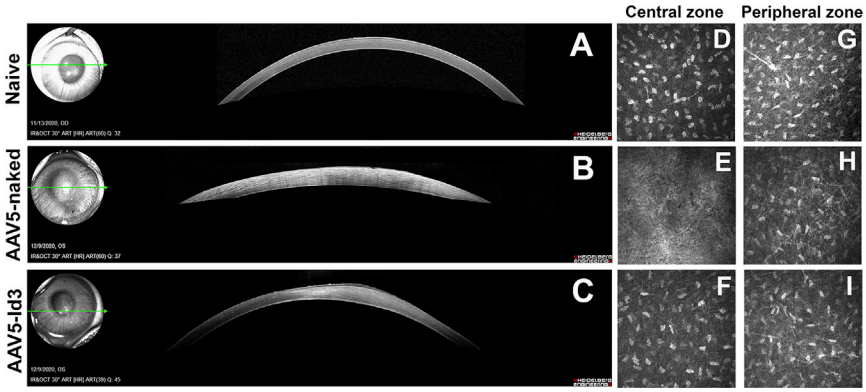

Figure 3. AAV5-Id3 gene therapy abolishes alkali trauma and conserves corneal integrity

(A–C) SPECTRALIS confocal images show that treatment with AAV5-Id3 minimized the fibrotic effects associated with alkali burn injury compared with AAV5-naked. A small strip of hyper-reflectivity was recorded in the anterior stroma and normal keratocyte density in AAV5-Id3-treated animals compared with AAV5-naked vector control group corneal tissues, which showed high reflectivity indicating the presence of haze post-alkali trauma on day 28. (D–F) Ultrastructural HRT3-RCM confocal images show that the AAV5-Id3 group cornea conserves the stromal keratocyte organization in the central stromal (injury) zone, while in the AAV5-naked vector group the keratocyte and basal nerve plexus were not visible in central stromal (injury) zone on day 28. (G–I) Ultrastructural HRT3-RCM confocal images of the peripheral corneal region (non-injury zone) show that the stromal keratocyte, extracellular matrix (ECM), and basal nerve plexus organization remain the same between the naive, AAV5-naked, and AAV5-Id3 group corneal tissues on day 28. All HRT3-RCM confocal images (D–I) are 400 × 400 μm.

compared with the AAV5-naked corneas (Figure 4E). Quantification showed a 23.78% ± 3.56% reduction of α-SMA in the AAV5-Id3 group compared with the AAV5-naked group ($p < 0.001$; Figure 4H). The collagen expression in naive, AAV5-naked, and AAV5-Id3 corneas was analyzed with Masson's trichrome staining (Figures 4I–4K). The stroma of the injured corneas (Figures 4I and 4J) showed higher collagen expression compared with the naive corneas (Figure 4K) while among two injured groups, AAV5-Id3 corneas (Figure 4J) showed markedly reduced collagen than the AAV5-naked corneas (Figure 4I). The quantification of collagen by measuring the pixel area of the blue color showed a 1.86 ± 0.27-fold reduction by AAV5-Id3 therapy (Figure 4I).

Quantity of delivered *Id3* gene copies

The amount of delivered *Id3* gene copies in corneas was quantified by real-time PCR following the published method.[19] Rabbit corneas treated with the AAV5-Id3 showed $4.12 \times 10^7 \pm 0.47$ copies of *Id3* per 1 μg of DNA (Figure S2); at the same time, AAV5-naked vector control group corneas showed *Id3* gene expression similar to that of naive control corneas.

Suitability of AAV5-Id3 gene therapy for the rabbit eye

To gauge the acceptance of AAV5-Id3 therapy, Modified MacDonald-Shadduck score, tear volume, central corneal thickness, and intraocular pressure (IOP) were measured in live rabbits in a time-dependent manner, and corneal tissue sections were subjected to hematoxylin and eosin (H&E) and immunofluorescence staining post euthanasia. The cumulative scores of the standard Draize and modified MacDonald-Shadduck tests recorded in live animals by two or more researchers in a blinded manner are presented in Table 1. As expected, both AAV-5 naked and AAV5-Id3 eyes showed significantly increased ($p < 0.001$) clinical scores up to day 3 in injured eyes compared with naive counterparts, owing to alkali wounding. From day 7 onward, the AAV5-Id3 gene therapy group animals' scores were reduced significantly ($p < 0.01$) compared with AAV5-naked group animals and trended toward those of naive control animals. Similar trends were observed at day 14 ($p < 0.05$) and day 21 ($p < 0.001$). No significant differences were detected in the central corneal thickness, IOP, or tear volume across time points between AAV5-Id3 and AAV5-naked groups, suggesting that the given AAV5-Id3 dosing does not result in iatrogenic corneal edema, ocular hypertension, or dry eye conditions (Figures 5A–5C).

Histological H&E staining showed no noticeable immune cell infiltration or foreign bodies in corneal tissue (Figures 6A–6C). In H&E, a mild aberration in morphology and presence of fibrosis/scarring was observed in AAV5-naked corneal sections attributable to the alkali injury while AAV5-Id3 therapy markedly attenuated these effects. CD11b (Figures 6D–6F) and F4/80 (Figures 6G–6I) immunofluorescence staining revealed unremarkable infiltration of immune cells in naive, AAV5-naked, and AAV5-Id3 corneal tissue sections. On a similar note, a TUNEL apoptosis assay detected few TUNEL-positive cells (<5) in the corneal stroma of all three groups (Figures 6J–6L), suggesting that AAV5-Id3 treatment is non-toxic and does not adversely affect keratocyte density. Detection of several TUNEL-positive cells in the corneal epithelium of all groups is due to physiological turnover of the squamous and wing cells of the epithelium. These results suggest that topical AAV5-Id3 treatment is tolerable for *in vivo* corneal therapeutic uses.

Association of Id3 with E-box protein

Our earlier *in vitro* studies showed regulation of E-box proteins by the *Id3* gene while reducing keratocyte differentiation.[23] Thus, we attempted to verify whether this mechanism is part of the anti-fibrotic response delivered by the AAV5-Id3 gene therapy in rabbit cornea *in vivo* using immunofluorescence and qRT-PCR techniques (Figure 7). The immunofluorescence analysis acknowledged the role of E-box proteins in corneal fibrosis, as increased E-box protein levels were detected in AAV5-naked corneas (Figure 7A) compared with naive corneas (Figure 7C) while AAV5-Id3-delivered corneas showed greatly decreased expression of E-box proteins (Figure 7B). The mRNA quantification data offered further support to this notion by showing significantly decreased mRNA expression of E2A (2.71 ± 0.47-fold; $p < 0.001$) and E2-2 (1.79 ± 0.41-fold; $p < 0.001$) genes in

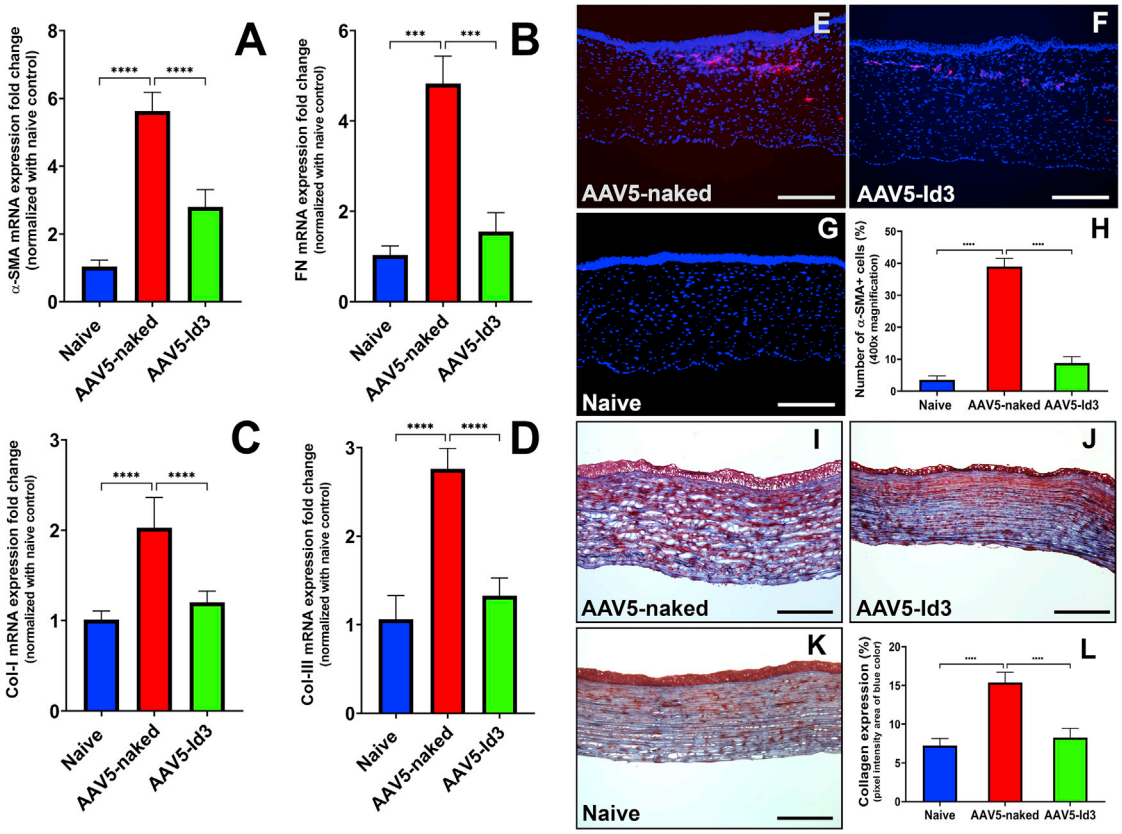

Figure 4. AAV5-Id3 gene therapy regulates profibrotic genes and regulates ECM organization

(A–D) qRT-PCR data reflect that AAV5-Id3 gene therapy attenuates the mRNA expression of profibrotic genes (α-smooth muscle actin (α-SMA], fibronectin [FN], collagen I [Col-I], and collagen III [Col-III], respectively) in corneal tissues compared with AAV5-naked vector control group corneal tissues on day 28. (E–G) Immunofluorescence staining of fibrosis marker α-SMA. Images of corneal tissue sections show that AAV5-Id3 gene therapy governs the fibrotic response at the protein level compared with AAV5-naked vector control group corneal tissues on day 28. (H) Quantification graph shows that AAV5-Id3 gene therapy significantly reduces the α-SMA level compared with AAV5-naked vector control group corneal tissues. (I–K) Masson's trichrome staining images of corneal tissue sections show that AAV5-Id3 gene therapy regulates collagen formation and maintains collagen-ECM organization compared with the AAV5-naked vector control group corneal tissues, as evident from a higher level of blue color intensity on day 28. (L) Quantification graph shows that AAV5-Id3 gene therapy significantly reduces the collagen level compared with AAV5-naked vector control group corneal tissues. Tissues were collected on day 28. There were six samples in each group, and error bars represent ±SEM. ***$p < 0.001$; ****$p < 0.0001$. Scale bars, 100 μm.

the AAV5-Id3 group compared with the AAV5-naked group (Figure 7D) and an unremarkable change in HEB mRNA levels in naive, AAV5-naked, and AAV5-Id3 groups (Figure 7D).

DISCUSSION

Previous studies have shown that Id proteins inhibit myofibroblast formation through bHLH class A and E proteins.[23–27] This study demonstrated that AAV5-mediated *Id3* gene therapy administered to the corneal stroma after alkali injury prevents corneal fibrosis formation and restores corneal transparency *in vivo* by attenuating TGF-β-mediated differentiation through E-box protein. Chemical, mechanical, and surgical insults to the cornea initiate a complex wound-healing response that promotes the upregulation of the endogenous corneal epithelial cell-derived cytokine TGF-β.[28] TGF-β is a multifunctional cytokine that contributes to a variety of pathophysiological processes involving cellular proliferation, differentiation, migration, and apoptosis.[29] In corneal injury, TGF-β plays a pivotal role in the wound-healing process by inducing the mesenchymal differentiation of activated keratocytes to myofibroblasts, which characteristically express α-SMA with contractile properties.[28–30] Under normal corneal wound-healing conditions, TGF-β expression returns to baseline levels and myofibroblasts are cleared from the healed wound bed through apoptosis. During aberrant corneal wound healing, TGF-β hyperactivity supports the generation of excessive and persistent myofibroblasts and the accumulation of excessive and disorganized extracellular matrix proteins, which contributes to the establishment of fibrotic lesions or scars.[31] The presence of a scar in the normally translucent cornea is a primary cause of decreased visual acuity following corneal injury. In addition to directing the transdifferentiation of activated keratocytes to myofibroblasts during the corneal wound-healing response, TGF-β interacts with a variety of transcription factors including, but not limited to, RUNX1, bHLH, and Ids.[23,24,32–34] bHLH and Ids also play an essential role in directing cellular fate by regulating the transcription of various genes.[24,35,36] *Id3* is implicated in the differentiation

Table 1. Draize and modified MacDonald-Shadduck scores showing ocular health assessment

	Draize cumulative score				Modified MacDonald-Shadduck cumulative score			
Groups	Baseline	Day 7	Day 14	Day 28	Baseline	Day 7	Day 14	Day 28
Naive	0	0	0	0	0	0	0	0
AAV5-naked	0	38.4 ± 3.06	28.3 ± 3.04	16.8 ± 3.07	0	1.21 ± 0.14	0.81 ± 0.08	0.67 ± 0.09
AAV5-Id3	0	12.8 ± 2.67	8.5 ± 2.51	3.9 ± 2.68	0	0.55 ± 0.11	0.48 ± 0.08	0.29 ± 0.12

The cumulative Draize and modified MacDonald-Shadduck scores showed significant differences in AAV5-Id3 group animals compared with AAV5-naked group counterparts ($p < 0.005$). Cumulative scores are presented as mean ± SEM.

of various stem/precursor cells into other cells during injury and wound healing. Ids are HLH transcriptional repressors that modulate multiple cellular processes including proliferation, migration, differentiation, and apoptosis in ocular and non-ocular tissue-derived cells.[24,32,37–40] Therefore, Ids could potentially be utilized to therapeutically modulate TGF-β overexpression and mitigate an aberrant wound-healing response following injury.

Currently, no effective therapies are available in clinics to treat corneal fibrosis without adverse side effects. We have reported several novel findings on wound healing, factors/genes, disease mechanisms, and development of novel therapies in preclinical animal models—*BMP7*, *Decorin*, *Id3*, and *Smad7* gene therapies, *BMP7* + *HGF* combination gene therapy, and two multimodal eye drops, SAHA and pirfenidone—and establishing their efficacy and short- and long-term safety.[4,5,19–21,24,28,29,41–47] Novel anti-fibrosis nanomedicine approaches that we have identified from cornea tissue were used to treat fibrosis in another ocular (conjunctiva) and non-ocular tissue (peritoneal) where fibrosis is a substantial clinical problem.[42,47] Our previous studies characterized the presence of Id proteins in ocular tissue and also uncovered the TGF-β-mediated and differentiation-related molecular mechanism *in vitro*.[23,24] We have demonstrated that *Id3* operates as a molecular switch and modulates TGF-β hyperactivity through interactions with the E-box protein.[24] This interaction between Id3 and TGF-β determines the cellular fate through temporal regulation of cellular proliferation and differentiation events during the corneal wound-healing process.

The known but previously unassociated mechanisms of Id3 and TGF-β in the wound-healing response prompted us to hypothesize that therapeutic overexpression of *Id3* through targeted gene therapy could be an ideal candidate for directing the corneal wound-healing response and ameliorating established corneal scars by inhibiting TGF-β. We have successfully delivered various candidate genes through AAV5-mediated viral vectors to inhibit TGF-β-mediated myofibroblast differentiation and reduce the expression of profibrogenic genes to minimize fibrosis in ocular and non-ocular tissues.[19,41–43]

In the present study, the time-dependent clinical evaluation and multimodal imaging of rabbit eyes demonstrated that delivery of the *Id3* gene into stromal fibroblasts via AAV5 significantly reduced corneal opacity at 28 days post alkali injury. These clinically significant findings indicate that topical AAV5-mediated *Id3* gene transfer following severe corneal trauma can mitigate corneal scarring and restore transparency. Furthermore, we also found through clinical evaluation with fluorescein staining that AAV5-mediated *Id3* gene transfer does not adversely influence the normal re-epithelialization process. Additionally, confocal imaging confirmed this observation at the ultrastructural level and supports that Id3 overexpression restores the corneal fibroblast arrangement and reduces inflammation and scarring.

The pro-wound-healing and anti-fibrotic effects of *Id3* gene therapy following severe corneal injury were further validated with a significant reduction in mRNA or protein levels of profibrotic genes including α-SMA, fibronectin, collagen type I, and collagen type III, suggesting that *Id3* overexpression inhibits TGF-β-induced corneal fibrosis in the rabbit. This is similar to our previous report that *Id3* is involved in the anti-fibrotic action of ITF2357 in rabbit corneal fibrosis.[44] Our findings were similar to those of previous reports that the administration of *Id2* or *Id3* suppresses lens epithelial cell injury-induced α-SMA and collagen generation in mice in eyes *in vivo* or inhibits the profibrotic activity of TGF-β and fibronectin in trabecular network cells in the human eye.[48,49] Additional evaluation with fluorescence microscopy highlighting the fibrosis marker α-SMA further corroborated our mRNA data.

The clinical evaluation of rabbit eyes in this study demonstrated that the overexpression of *Id3* attenuated corneal fibrosis and the wound-healing process without any adverse effects on normal ocular pressure or tear production levels, similar to a previous study reporting that *Id3* is implicated in inhibiting TGF-β-induced IOP in mouse eyes.[50] In addition, evaluation employing the Draize ocular irritancy criteria and modified MacDonald-Shadduck scoring system indicates that ocular toxicity stemming from topical AAV5-Id3 administration is negligible, as reported in Table 1. Furthermore, using CD11b, a pan-myeloid/leukocyte marker, and F4/80, a macrophage marker, immunofluorescence was performed to evaluate immunogenicity of AAV5-Id3 gene therapy to corneal tissue. CD11b is expressed on many immune cells of myeloid lineages such as monocytes, macrophages, and granulocytes while F4/80 is a general macrophage marker. We did not evaluate cell-specific markers against individual immune cells, as no clinically relevant inflammation was observed during slit-lamp examination in rabbit eyes *in vivo* after gene therapy. These observations indicate that AAV5-Id3 gene therapy does not induce inflammation and is non-immunogenic to the cornea. After

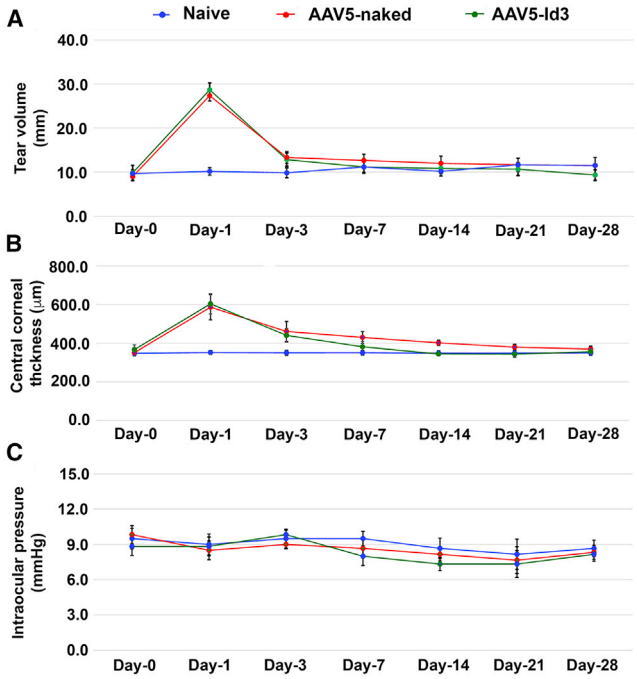

Figure 5. Corneal physiological parameters were not compromised during AAV5-Id3 gene therapy to the corneal tissues

(A) Schirmer tear test graph shows that AAV5-Id3 gene therapy does not vary the normal secretion of ocular flow compared with the naive and AAV5-naked vector groups. The tear flow manifestly increased after day 1 and reverted to normal on day 3 in well-defined limitation of topical gene therapy. (B) Pachymetry graph shows that corneal thickness was constant throughout the study in a time-dependent manner in naive, AAV5-naked, and AAV5-Id3 corneal tissue groups. The corneal thickness increased after day 1 and reverted to normal on day 7 in well-defined limitation of topical gene therapy. (C) Tonometry graph shows that intraocular pressure (IOP) is not a potential concern of AAV5-Id3 gene therapy. The IOP was constant and within the normal range in naive, AAV5-naked, and AAV5-Id3 groups of animals in a time-dependent manner. There were six samples in each group, and error bars represent ±SEM.

administration, the *Id3* gene remained in the injured rabbit cornea for up to 4 weeks with no deleterious morphological changes, inflammation, or cytotoxicity as determined through corneal histology, CD11b staining, F4/80 staining, and TUNEL apoptosis assay. These data are consistent with those of our previous report whereby *Id3* overexpression did not cause any cytotoxicity in human corneal stromal fibroblasts (hCSFs), and inhibits α-SMA expression and differentiation of hCSFs *in vitro* through E2A protein.[23] The present study revealed that HLH proteins, Id3, and E-box proteins can form hetero-oligomeric complexes that modulate the cellular differentiation cascade. These findings corroborate previous reports which demonstrate the ability of Id proteins to inhibit myofibroblast formation through association with bHLH class A and E proteins including E12, E47, E2-2, and HEB.[23,38,44–53]

A previous report indicates that *Id3* inhibits scar-associated collagen production from fibroblasts that are implicated in fibrosis.[54] The current study suggests that *Id3* suppresses corneal myofibroblast differentiation through control of the bHLH protein. This proposed mechanism whereby Id3 interacts directly with the bHLH protein or prevents the interaction of E2A proteins has been previously demonstrated in studies involving preadipocytes.[33] Our results were well aligned with the findings of ocular and non-ocular tissue investigations showing that *Id3* regulates TGF-β-mediated profibrotic pathways and establishes the direct role of *Id3* with bHLH- and E-box-driven differentiations.[48–56]

This study supports our previous findings that suggested a mechanistic role for *Id3* and E-box proteins during TGF-β-induced fibroblast to myofibroblast differentiation but did not conclude a causal relationship, localization, nuclear-cytoplasmic shuttling of *Id3*, and stimulus of E-box proteins.[23,24] Our future studies will address these limitations by categorizing the mechanistic and functional influence of *Id3* and E-box proteins on fibroblast proliferation, differentiation, and fate.

To our knowledge, this is the first study to demonstrate that the transcription factor Id3 regulates fibrosis following injury and serves to maintain corneal transparency *in vivo*. This innovative approach utilizing localized *Id3* overexpression is anticipated to foster the development of tissue-targeted gene therapies to resolve pre-existing corneal fibrosis safely and efficiently without additional surgical procedures.

The long-term safety and tolerability of AAV5-mediated *Id3* gene transfer on stromal keratocyte density and anterior segment morphology are unknown and represent the limitations of our current investigation. These will be evaluated with *in vivo* confocal microscopy and OCT in cross-sectional and longitudinal studies in the future.

Clinical eye evaluations demonstrated a time-dependent resolution of corneal opacity following *Id3* gene therapy. However, molecular analysis revealed a trend for profibrotic genes to remain slightly elevated across time points following corneal injury in AAV5-Id3-treated corneas compared with naive corneas. This multidimensional therapeutic approach to targeting different fibrotic signaling pathways in the corneal wound-healing process may offer the potential to completely abolish persistent subclinical haze represented by mildly elevated expression of profibrotic genes.

In conclusion, this study demonstrated that AAV5-mediated *Id3* gene therapy administered locally to the corneal stroma after alkali insult eliminates corneal fibrosis and restores transparency *in vivo* by attenuating TGF-β-induced directed myofibroblast differentiation through interactions with the E-box protein.

MATERIALS AND METHODS

Chemicals and reagents

Standard research-grade chemicals and reagents were used to perform this study. In brief, topical artificial tears were purchased from the Rugby Laboratories (Livonia, MI). Sterile Weck-Cel ophthalmic spears were purchased from Beaver-Visitec International

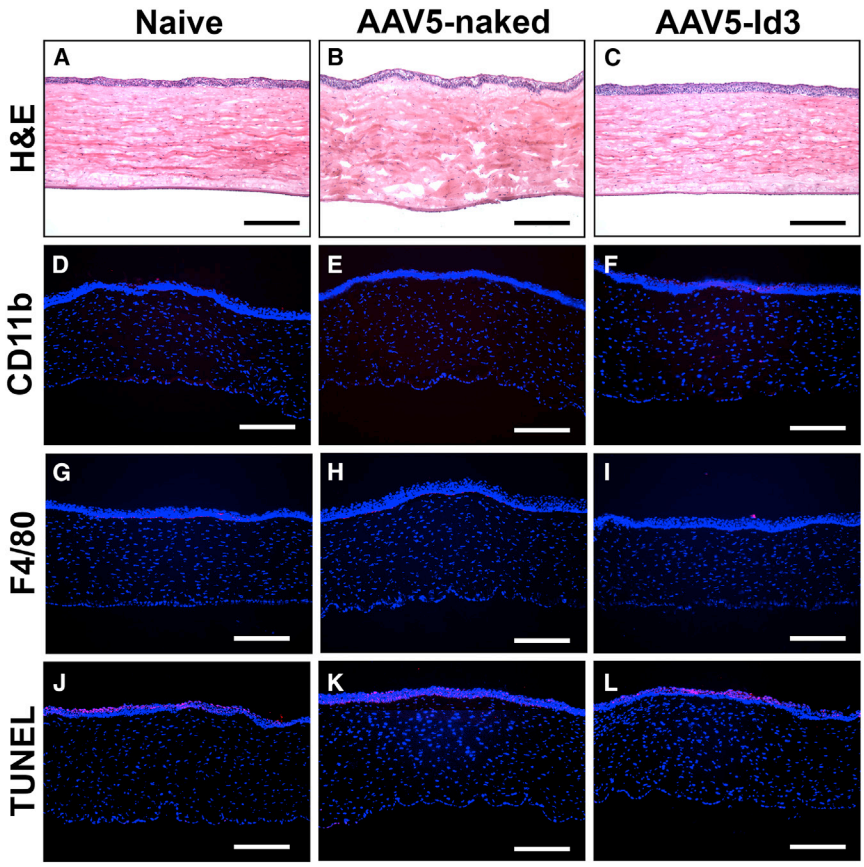

Figure 6. AAV5-Id3 gene therapy is adequate for rabbit corneal tissue

(A–C) H&E staining images show that no noticeable alterations were recorded in gross morphology of corneal tissue anatomy after AAV5-Id3 gene therapy corneal tissue sections compared with naive and AAV5-naked vector control group corneal sections. No infiltration of macrophages, neutrophils, and external bodies appeared in any tissue sections. (D–F) CD11b immunofluorescence staining images confirm that no macrophages/integrins were recorded after AAV5-Id3 gene therapy in corneal tissue sections compared with naive and AAV5-naked vector control groups in corneal sections. (G–I) F4/80 immunofluorescence staining images confirm that no macrophage infiltrations were recorded after AAV5-Id3 gene therapy in corneal tissue sections compared with naive and AAV5-naked vector control groups in corneal sections. (J–L) TUNEL apoptosis staining images confirm that AAV5 Id3 gene therapy shows no apoptosis in the corneal stromal region. The TUNEL$^+$ cells (apoptotic/necrotic) appear in the outer squamous and wing cells and are part of the regular turnover process of corneal epithelial cells, and are consistent in naive, AAV5-naked vector, and AAV5-Id3 gene therapy corneal tissue sections. Tissues were collected on day 28. Scale bars, 100 μm.

(Waltham, MA). Surgical forceps, wire speculum, and sharp Westcott scissors were purchased from World Precision Instruments (Sarasota, FL). Ketamine hydrochloride (JHP Pharmaceuticals, Rochester, MI), xylazine hydrochloride (XylaMed, Bimeda, Oakbrook Terrace, IL), 0.5% proparacaine hydrochloride (Alcon, Fort Worth, TX), BSS (Alcon), and pentobarbital (Diamondback Drugs, Scottsdale, AZ) were obtained from the pharmacy of the Harry S. Truman VA Medical Center (Columbia, MO). H&E solutions were procured from StatLab Medical Products (McKinney, TX). 2-Methyl butane (Thermo Fisher, Waltham, MA) and anti-fade mounting medium containing 4′,6-diamidino-2-phenylindole dihydrochloride (DAPI) (H1200; Vector Laboratories, Burlingame, CA) were obtained from commercial vendors.

Animals

All animals were treated according to the Association for Research in Vision and Ophthalmology Statement for the Use of Animals in Ophthalmic and Vision Research. The Institutional Animal Care and Use Committees (IACUC) of the University of Missouri and the Harry S. Truman Memorial Veterans' Hospital approved the study. Twenty-four 2- to 3-month-old male and female New Zealand White rabbits (Charles River Laboratory, Wilmington, MA) weighing 2.5–3.0 kg, were used in this study to avoid any sex-variable impact.[57] During the procedure the animals were anesthetized by intramuscular injection of a mixture of ketamine hydrochloride (50 mg/kg) and xylazine hydrochloride (10 mg/kg). In addition, ophthalmic 0.5% proparacaine hydrochloride was topically applied to the corneas for local anesthesia before any procedure. Eyes were kept moist with topical artificial tears during anesthetic events to prevent corneal desiccation.

Generation of AAV5-Id3

The *Id3* gene was PCR-amplified from rabbit corneal fibroblast cDNA and cloned into the AAV5 plasmid pTRUF11. The expression cassette contained a hybrid promoter (cytomegalovirus enhancer and chicken β-actin promoter) and the simian virus 40 polyadenylation site. Multiple clones were sequenced to rule out any potential mutations introduced during PCR. Recombinant AAV5-Id3 virus was generated by the Gene Therapy Core, University of Florida (Gainesville, FL) using a two-plasmid co-transfection packaging method as previously reported.[19,41–43,45]

Corneal scarring and transduction of AAV5-Id3

Corneal scarring was induced in one eye of each rabbit, and the contralateral eye served as a naive control. To induce corneal scarring, rabbits were anesthetized before the procedure, and an alkali-treated filter paper (8 mm, soaked in 0.5 N sodium hydroxide solution) was placed onto the central cornea for 30 s with the aid of a surgical microscope (Leica Wild Microscope MEL53; Leica, Wetzlar, Germany). The wounded corneas were immediately and copiously rinsed with sterile BSS to remove residual alkali solution. This standardized method of

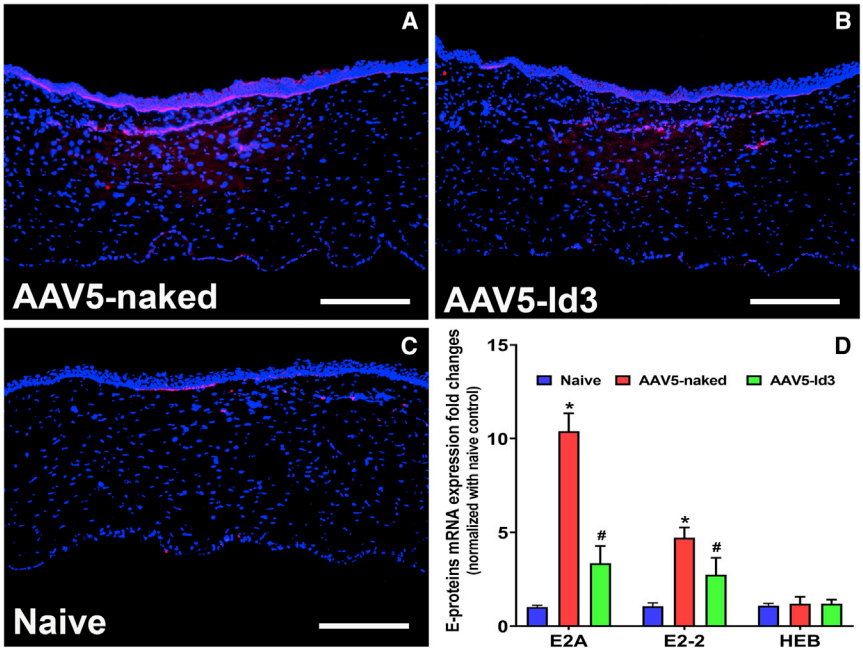

Figure 7. AAV5-Id3 gene therapy regulates corneal fibrosis through E-box proteins

(A–C) Decreased level of expression of E-box proteins (E2A, E2-2, and HEB) in immunofluorescence images of corneal tissue sections of the AAV5-Id3 group confirmed that Id3 regulates the fibrotic response via E-box protein compared with AAV5-naked vector control group corneal tissue sections. The used E2A antibody detected the E2A and E2A isoforms E12 and HEB. (D) Quantification graph shows that AAV5-Id3 gene therapy significantly reduces the mRNA expressions of E2-A and E2-2 genes compared with AAV5-naked vector control group corneal tissues, and at the same time the HEB expression levels were not impacted in naive, AAV5-naked, and AAV5-Id3 corneal tissues. Tissues were collected on day 28. There were six samples in each group, and error bars represent ±SEM. *$p < 0.001$; #$p < 0.01$. Scale bars, 100 μm.

injury triggered wound healing and produced dense corneal scarring and peak fibrosis at 3–4 weeks as reported previously.[20]

The AAV5-Id3 transduction was administered to the corneal stroma with epithelial debridement 24 h after alkali injury with our customized cloning cylinder method as reported previously.[19,41–43,45] The animals were divided into four groups. Group I corneas were exposed topically to 100 μL of AAV5-Id3 titer (6.5×10^{12} μg/mL) for 5 min via a custom cloning cylinder technique after alkali injury (AAV5-Id3 group). Group II corneas received 100 μL of AAV5-naked titer (3.8×10^{12} μg/mL) as detailed above (AAV5-naked group). Group III corneas from contralateral eyes represented naive corneas and served as a naive control (naive group). Group IV corneas from contralateral eyes represented naked AAV5 only and served as a negative control (vector control group). Our earlier study found that not showing inflammatory response 4 weeks after the alkali injury (0.5 M) used in the study was noteworthy.[20] Therefore, in this study, as per the IACUC guidelines following the 3R rule of the American Association for Laboratory Animal Care, we have used the contralateral eyes as naive controls. In brief, corneal epithelium was debrided by gentle scraping with a #64 Beaver blade (BD Biosciences, Franklin Lakes, NJ) and the AAV5-Id3 gene was delivered to an anesthetized rabbit. Under a surgical microscope, a wire eyelid speculum (10 × 4 mm) was inserted to expose the corneal surface for customized gene delivery into the corneal stroma. Proparacaine hydrochloride solution (0.5% solution, 2–3 drops) was topically applied before the procedure.

Clinical assessment and live biomicroscopy

Slit-lamp microscopy and haze quantification

To minimize variations, the level of corneal haze and gross ocular health in anesthetized rabbits was evaluated through visual clinical examination including slit-lamp microscopy at regular intervals before and after gene therapy (1, 3, 7, 14, 21, and 28 days) as reported previously.[19,20,45,57–59] A slit-lamp microscope (SL-15 portable slit-lamp; Kowa, Torrance, CA) fitted with a high-definition digital imaging system (portable VK-2 Ver. 5.50; Kowa) was used to record clinical ocular health assessment data. A stereomicroscope (Leica MZ16F; Leica Microsystems, Buffalo Grove, IL) equipped with a digital camera (SpotCam RT KE; Diagnostic Instruments, Sterling Heights, MI) was used to assess and record the effect of gene therapy progression in a time-dependent manner for haze evaluation using the Fantes scale.[19,20,45] The intensity of corneal haze as documented by the images was graded by a minimum of three independent observers (S.G., E.A.G., L.M.M., N.P.H., or R.R.M.) masked to the treatment group, as reported earlier.[19,20,45] In brief, the grading system was the following: grade 0, completely clear cornea; grade 0.5, trace haze seen with careful oblique illumination; grade 1, more obvious haze but not interfering with the visualization of fine iris details; grade 2, mild obscuration of iris details; grade 3, moderate obscuration of the iris and lens; and grade 4, complete opacification of the stroma in the area of ablation. *In vivo*, clinical examinations were performed by at least two independent observers (S.G., E.A.G., L.M.M., N.P.H., or R.R.M.) in a blinded manner.[19,20,45]

Fluorescein eye test for the assessment of corneal epithelial health

Corneal epithelial defects were observed with a topically applied commercial ophthalmic fluorescein stain (Altafluor Benox). The epithelial defects were assessed under a cobalt light blue filter and recorded under a GFP light filter using a slit-lamp microscope equipped with an image-capturing system (Leica MZ16F) using a digital camera (SpotCam RT KE). The clinical findings were documented by photography and the images were scored by a minimum of two independent observers (S.G., E.A.G., L.M.M., N.P.H., or R.R.M.) in a blinded fashion. The size of corneal epithelial defects in rabbit eyes was

digitally computed by counting pixels of the defect areas in images taken with a stereomicroscope at 7.1× magnification using ImageJ and Photoshop software following the procedure reported earlier.[20]

Intraocular pressure, corneal thickness, and tear production

Administration of therapeutic genes into the corneal stroma has the potential to induce secondary alterations in aqueous humor production or in tissues of the anterior chamber, which is a significant concern after gene therapy. During the entire study the variations in IOP, corneal thickness, and ocular discharge were recorded in a time-dependent manner. The IOP measurements in rabbit eyes were recorded using a tonometer (Tono-Pen AVIA; Reichert Technologies, Depew, NY, USA); the corneal thickness was recorded using an ultrasonic pachymeter (AccuPach VI Pachymeter; Accutome, Malvern, PA) to assess corneal thickness; and tear production was recorded using Schirmer tear test strips (Fisher Scientific) at regular timed intervals on days 1, 3, 7, 14, 21, and 28 and before each clinical biomicroscopy evaluation as reported previously.[20,41,43,53] To avoid the normal diurnal variation and operator variability, all measurements were performed between 9 AM and noon by one observer (S.G.).

Live ultrastructural assessment using confocal microscopy

Confocal microscopy was employed to capture serial images of the cornea at different depths in a real-time manner. The high-resolution confocal imaging systems SPECTRALIS (Heidelberg Engineering, Dossenheim, Germany) Anterior Segment Module and HRT3-RCM (Heidelberg Engineering) were used to record the corneal details and assessment of overall corneal anatomy at an ultrastructural level as detailed previously.[41,43]

Draize and modified MacDonald-Shadduck eye test

The ocular health and anomalies were evaluated independently at selected times by at least three observers (S.G., E.A.G., L.M.M., N.P.H., or R.R.M.) using the established Draize and modified MacDonald-Shadduck ocular scoring assessments. The Draize eye test became a governmentally endorsed method to evaluate the safety of materials for use in or around the eyes. The test involves a standardized protocol for instilling agents onto the cornea and conjunctiva of laboratory animals. A sum of ordinal-scale items of the outer eye gives an index of ocular morbidity.[20,60] Additionally, the ocular health was also assessed with a modified MacDonald-Shadduck ocular scoring system for detailed evaluation of the AAV5-Id3 gene therapy in corneal tissue as reported earlier.[20,61]

Corneal tissue collection

At the termination point of the study, the rabbits were humanely euthanized with an intravenous injection of pentobarbital (150 mg/kg) while animals were under general anesthesia. Eyes were enucleated with surgical forceps and Westcott scissors under a dissecting microscope (Leica Wild M690; Leica Microsystems). The corneal tissues were immediately placed into molds containing optimal cutting temperature compound and snap-frozen in a container of 2-methyl butane immersed in liquid nitrogen or directly placed into cryovials and immersed in liquid nitrogen for molecular analysis at mRNA level. Frozen tissues were maintained at −80°C until sectioning and further evaluation. Optimal cutting temperature embedding of unfixed tissue was also done for subsequent immunostaining analysis of sections. Tissues were sectioned at 8-μm thickness with a cryomicrotome, mounted on glass microscopic slides, and preserved at −80°C for subsequent analysis.

Extraction of mRNA, cDNA synthesis, and quantitative real-time PCR

RNeasy kit (Qiagen, Valencia, CA) was used to extract mRNA from rabbit corneal tissues and reverse transcribed into cDNA using a commercial kit (Promega, Madison, WI) following the vendor's instructions. qRT-PCR was performed using an All-in-One qPCR mix (GeneCopoeia, Rockville, MD) according to the vendor's instructions. In brief, each 20-μL reaction contained 10 μL of 2× All-in-One qPCR mix, 2 μL of cDNA (0.5 μg), 2 μL of forward primer (0.2 μM), 2 μL of reverse primer (0.2 μM), and 4 μL of RNase and DNase free water. The reaction ran at universal cycle (95°C for 3 min, 40 cycles of 95°C for 30 s, followed by 60°C for 60 s) following the published protocol.[42,46,57,59,62] The nucleotide sequences of primers (forward and reverse) used for amplification in this study are provided in Table S1. Beta-actin (*β-actin*) was used as a housekeeping gene to normalize the qRT-PCR data and verify the quality of cDNA. The threshold cycle (Ct) was used to detect the increase in the signal associated with the exponential growth of PCR product during the log-linear phase. The relative mRNA expression was calculated using the $2^{\Delta\Delta Ct}$ method and reported as a fold change relative to the corresponding control values.

Histology and fluorescence microscopy

H&E staining and Masson's trichrome staining

The rabbit corneal tissue sections of all the groups were subjected to H&E staining for the assessment of morphological alterations. H&E staining was performed in our laboratory using the protocol reported previously.[20,53] Additionally, corneal sections were also sent to the Veterinary Medical Diagnostic Laboratory (VMDL) at the University of Missouri College of Veterinary Medicine for H&E histology.

Similarly, for the assessment of alterations in collagen content, a primary component of the extracellular matrix, corneas underwent Masson's trichrome staining at the VMDL using an established protocol.[20,58]

Characterization of fibrotic protein using immunofluorescence microscopy

The changes in levels of fibrotic proteins were recorded using a myofibroblast marker, α-SMA. The mouse monoclonal antibody was used for α-SMA (Dako, Agilent Technologies, Santa Clara, CA), to capture the changes in profibrotic protein levels as reported earlier.[19–21] In brief, the rabbit corneal tissue sections were washed twice with 1× PBS (5 min each), followed by blocking with 2% serum (30 min at room temperature), and finally incubated with primary antibody at a 1:100 dilution for 90 min at room

temperature. The tissue sections were washed three times with 1× PBS (5 min each) and conjugated with secondary antibody Alexa Fluor 594 goat anti-mouse IgG (Invitrogen, Molecular Probes, Life Technologies, Eugene, OR) at a dilution of 1:500 for 1 h. Tissues were mounted with Vectashield containing DAPI (Vector Laboratories) for the visualization of nuclei. Irrelevant isotype-matched primary antibody, secondary antibody alone, and tissue sections from naive eyes were used as negative controls. Stained cells were visualized under a Leica fluorescence microscope and photographed with a digital camera (SpotCam RT KE).

Safety and tolerability of AAV5-Id3 gene therapy in corneal tissue

The possibility of immunologic reaction and cytotoxicity of AAV5-Id3 gene therapy was evaluated by performing CD11b (BDB550 282; BD Pharmingen, San Jose, CA), F4/80 (SC-377009; Santa Cruz Biotechnology, Dallas, TX), and TUNEL (ApopTag; Millipore, Burlington, MA) immunostaining in rabbit corneal sections. For CD11b staining, corneal tissue sections were incubated at room temperature with the primary antibody at a 1:100 dilution in a 1× HEPES buffer containing 2% BSA for 90 min, followed by goat anti-rat IgG secondary antibody (Alexa Fluor 594; Invitrogen) at a 1:500 dilution for 60 min. After completion of immunostaining, tissue sections were mounted in a medium containing DAPI (Vectashield), viewed, and photographed under a fluorescence microscope (Leica, Deerfield, IL) equipped with a digital camera system (SpotCam RT KE).[19,20,45] For the TUNEL assay to detect the apoptotic cells, tissue sections were fixed in 1% paraformaldehyde at room temperature followed by subsequent permeabilization with ethanol/acetic acid (2:1 ratio; at −20°C) and treated with fluorescent detection assay kit reagents to detect apoptosis and/or necrosis according to the manufacturer's instructions and as reported previously.[19–21]

E-box proteins driving AAV5-Id3-mediated anti-fibrotic response

For characterization of the role of E-box proteins in AAV5-Id3-mediated anti-fibrotic response in the corneal tissue, E2A immunofluorescence staining was performed using the E2A antibody (SC-416; SCBT, Santa Cruz Biotechnology). The E2A antibody is recommended for the detection of E2A and E2A isoforms E12 and HEB. Corneal tissue sections were incubated at room temperature with the primary antibody at a 1:100 dilution in a 1× HEPES buffer containing 2% BSA for 90 min, followed by Alexa Fluor 594 goat anti-mouse IgG (Invitrogen). After completion of immunostaining, tissue sections were mounted in a medium containing DAPI (Vectashield), viewed, and photographed under a fluorescence microscope (Leica) equipped with a digital camera system (SpotCam RT KE).[23]

Statistical analysis

Statistical analysis was performed using one-way ANOVA followed by a post hoc Bonferroni multiple comparison test for clinical and molecular data assessment. The average results were expressed with a standard error of the mean (±SEM). Statistical significance was considered if $p < 0.05$.

SUPPLEMENTAL INFORMATION

Supplemental information can be found online at https://doi.org/10.1016/j.ymthe.2022.06.018.

ACKNOWLEDGMENTS

This work was primarily supported by the 1I01BX000357, Veteran's Health Affairs Merit and Research Career Scientist grants (R.R.M.), Washington, DC; and partially by the NIH/NEI 5R01EY017294, 5R01EY030774, and 1U01EY031650 grants (R.R.M.), Bethesda, MD, and the Ruth Kraeuchi Missouri Endowed Chair Ophthalmology Fund (R.R.M.), University of Missouri, Columbia, MO.

AUTHOR CONTRIBUTIONS

S.G. performed experiments, data collection, and statistical analysis, and prepared the draft of the manuscript. M.K.F. assisted with draft preparation. D.K. assisted with editing of the manuscript. N.R.S. assisted with immunofluorescence and qRT-PCR studies. L.M.M. assisted in data review and manuscript drafting. L.M.K. assisted with immunofluorescence and qRT-PCR studies. P.R.S. assisted with immunofluorescence and qRT-PCR studies. E.A.G. helped during clinical observations, provided important feedback, and assisted in manuscript improvement. N.P.H. helped during clinical observations, and assisted in manuscript improvement. S.P.R. re-cloned the Id3 gene into AAV-pTRUF11 plasmid. S.S.C. assited in data analysis/interpetation. R.R.M. conceived the idea, supervised experiments, arranged for resources, helped during clinical observations, made critical improvements, and finalized the manuscript.

DECLARATION OF INTERESTS

The authors declare no competing interests.

REFERENCES

1. Imanishi, J., Kamiyama, K., Iguchi, I., Kita, M., Sotozono, C., and Kinoshita, S. (2000). Growth factors: importance in wound healing and maintenance of transparency of the cornea. Prog. Retin. Eye Res. *19*, 113–129.
2. Torres, P.F., and Kijlstra, A. (2001). The role of cytokines in corneal immunopathology. Ocul. Immunol. Inflamm. *9*, 9–24.
3. Li, M., Huang, H., Li, L., He, C., Zhu, L., Guo, H., Wang, L., Liu, J., Wu, S., Liu, J., et al. (2021). Core transcription regulatory circuitry orchestrates corneal epithelial homeostasis. Nat. Commun. *12*, 420.
4. Shetty, R., Kumar, N.R., Subramani, M., Krishna, L., Murugeswari, P., Matalia, H., Khamar, P., Dadachanji, Z.V., Mohan, R.R., Ghosh, A., and Das, D. (2021). Safety and efficacy of the combination of suberoylamilide hydroxyamic acid and mitomycin C in reducing pro-fibrotic changes in human corneal epithelial cells. Sci. Rep. *11*, 4392.
5. Anumanthan, G., Sharma, A., Waggoner, M., Hamm, C.W., Gupta, S., Hesemann, N.P., and Mohan, R.R. (2017). Efficacy and safety comparison between suberoylanilide hydroxamic acid and mitomycin C in reducing the risk of corneal haze after PRK treatment *in vivo*. J. Refract. Surg. *33*, 834–839.
6. Miller, D.D., Hasan, S.A., Simmons, N.L., and Stewart, M.W. (2019). Recurrent corneal erosion: a comprehensive review. Clin. Ophthalmol. *13*, 325–335.
7. Feizi, S., Azari, A.A., and Safapour, S. (2017). Therapeutic approaches for corneal neovascularization. Eye Vis. *4*, 28.
8. Arranz-Marquez, E., Katsanos, A., Kozobolis, V.P., Konstas, A.G.P., and Teus, M.A. (2019). A critical overview of the biological effects of mitomycin C application on the cornea following refractive surgery. Adv. Ther. *36*, 786–797.
9. Mearza, A.A., and Aslanides, I.M. (2007). Uses and complications of mitomycin C in ophthalmology. Expert Opin. Drug Saf. *6*, 27–32.

10. Berthelier, V., Laigle, A., Jollès, B., and Chinsky, L. (1995). Distortion after monofunctional alkylation by mitomycin C of a dodecamer containing its major binding site. J. Biomol. Struct. Dyn. *12*, 899–910.

11. Jollès, B., and Laigle, A. (1995). Mitomycin C-induced distortions of DNA at minor alkylation sites. Chem. Biol. Interact. *94*, 215–224.

12. Shukla, S., Mittal, S.K., Foulsham, W., Elbasiony, E., Singhania, D., Sahu, S.K., and Chauhan, S.K. (2019). Therapeutic efficacy of different routes of mesenchymal stem cell administration in corneal injury. Ocul. Surf. *17*, 729–736.

13. Singh, V., Tiwari, A., Kethiri, A.R., and Sangwan, V.S. (2021). Current perspectives of limbal-derived stem cells and its application in ocular surface regeneration and limbal stem cell transplantation. Stem Cell. Transl. Med. *10*, 1121–1128.

14. Sahu, A., Foulsham, W., Amouzegar, A., Mittal, S.K., and Chauhan, S.K. (2019). The therapeutic application of mesenchymal stem cells at the ocular surface. Ocul. Surf. *17*, 198–207.

15. Singh, R., Gupta, N., Vanathi, M., and Tandon, R. (2019). Corneal transplantation in the modern era. Indian J. Med. Res. *150*, 7–22.

16. Gain, P., Jullienne, R., He, Z., Aldossary, M., Acquart, S., Cognasse, F., and Thuret, G. (2016). Global survey of corneal transplantation and eye banking. JAMA Ophthalmol. *134*, 167–173.

17. Röck, T., Landenberger, J., Bramkamp, M., Bartz-Schmidt, K.U., and Röck, D. (2017). The evolution of corneal transplantation. Ann. Transpl. *22*, 749–754.

18. Yu, T., Rajendran, V., Griffith, M., Forrester, J.V., and Kuffová, L. (2016). High-risk corneal allografts: a therapeutic challenge. World J. Transpl. *6*, 10–27.

19. Gupta, S., Rodier, J.T., Sharma, A., Giuliano, E.A., Sinha, P.R., Hesemann, N.P., Ghosh, A., and Mohan, R.R. (2017). Targeted AAV5-Smad7 gene therapy inhibits corneal scarring *in vivo*. PLoS One *12*, e0172928.

20. Gupta, S., Fink, M.K., Ghosh, A., Tripathi, R., Sinha, P.R., Sharma, A., Hesemann, N.P., Chaurasia, S.S., Giuliano, E.A., and Mohan, R.R. (2018). Novel combination BMP7 and HGF gene therapy instigates selective myofibroblast apoptosis and reduces corneal haze *in vivo*. Invest. Ophthalmol. Vis. Sci. *59*, 1045–1057.

21. Tandon, A., Sharma, A., Rodier, J.T., Klibanov, A.M., Rieger, F.G., and Mohan, R.R. (2013). BMP7 gene transfer via gold nanoparticles into stroma inhibits corneal fibrosis *in vivo*. PLoS One *8*, e66434.

22. Ito, Y., and Miyazono, K. (2003). RUNX transcription factors as key targets of TGF-beta superfamily signaling. Curr. Opin. Genet. Dev. *13*, 43–47.

23. Gupta, S., Martin, L.M., Sinha, N.R., Smith, K.E., Sinha, P.R., Dailey, E.M., Hesemann, N.P., and Mohan, R.R. (2020). Role of inhibitor of differentiation 3 gene in cellular differentiation of human corneal stromal fibroblasts. Mol. Vis. *26*, 742–756.

24. Mohan, R.R., Morgan, B.R., Anumanthan, G., Sharma, A., Chaurasia, S.S., and Rieger, F.G. (2016). Characterization of Inhibitor of differentiation (Id) proteins in human cornea. Exp. Eye Res. *146*, 145–153.

25. Murre, C. (2019). Helix-loop-helix proteins and the advent of cellular diversity: 30 years of discovery. Genes Dev. *33*, 6–25.

26. Massari, M.E., and Murre, C. (2000). Helix-loop-helix proteins: regulators of transcription in eukaryotic organisms. Mol. Cell. Biol. *20*, 429–440.

27. Tarczewska, A., and Greb-Markiewicz, B. (2019). The Significance of the intrinsically disordered regions for the functions of the bHLH transcription factors. Int. J. Mol. Sci. *20*, 5306.

28. Tandon, A., Tovey, J.C.K., Sharma, A., Gupta, R., and Mohan, R.R. (2010). Role of transforming growth factor-beta in corneal function, biology, and pathology. Curr. Mol. Med. *10*, 565–578.

29. Kamil, S., and Mohan, R.R. (2021). Corneal stromal wound healing: major regulators and therapeutic targets. Ocul. Surf. *19*, 290–306.

30. Ljubimov, A.V., and Saghizadeh, M. (2015). Progress in corneal wound healing. Prog. Retin. Eye Res. *49*, 17–45.

31. Shu, D.Y., and Lovicu, F.J. (2017). Myofibroblast transdifferentiation: the dark force in ocular wound healing and fibrosis. Prog. Retin. Eye Res. *60*, 44–65.

32. Barone, M.V., Pepperkok, R., Peverali, F.A., and Philipson, L. (1994). Id proteins control growth induction in mammalian cells. Proc. Natl. Acad. Sci. USA *91*, 4985–4988.

33. Moldes, M., Lasnier, F., Fève, B., Pairault, J., and Djian, P. (1997). Id3 prevents differentiation of preadipose cells. Mol. Cell. Biol. *17*, 1796–1804.

34. Kinoshita, K., Iimuro, Y., Otogawa, K., Saika, S., Inagaki, Y., Nakajima, Y., Kawada, N., Fujimoto, J., Friedman, S.L., and Ikeda, K. (2007). Adenovirus-mediated expression of BMP-7 suppresses the development of liver fibrosis in rats. Gut *56*, 706–714.

35. Izumi, N., Mizuguchi, S., Inagaki, Y., Saika, S., Kawada, N., Nakajima, Y., Inoue, K., Suehiro, S., Friedman, S.L., and Ikeda, K. (2006). BMP7 opposes TGF-beta1-mediated collagen induction in mouse pulmonary fibroblasts through Id2. Am. J. Physiol. Lung Cell. Mol. Physiol. *290*, L120–L126.

36. Veerasamy, M., Phanish, M., and Dockrell, M.E.C. (2013). Smad mediated regulation of inhibitor of DNA binding 2 and its role in phenotypic maintenance of human renal proximal tubule epithelial cells. PLoS One *8*, e51842.

37. Roschger, C., and Cabrele, C. (2017). The id-protein family in developmental and cancer-associated pathways. Cell Commun. Signal. *15*, 7.

38. Ling, F., Kang, B., and Sun, X.H. (2014). Chapter five: id proteins. Small molecules, mighty regulators. Curr. Top. Dev. Biol. *110*, 189–216.

39. Atherton, G.T., Travers, H., Deed, R., and Norton, J.D. (1996). Regulation of cell differentiation in C2C12 myoblasts by the Id3 helix-loop-helix protein. Cell Growth Differ. *7*, 1059–1066.

40. Jen, Y., Manova, K., and Benezra, R. (1997). Each member of the Id3 gene family exhibits a unique expression pattern in mouse gastrulation and neurogenesis. Dev. Dyn. *208*, 92–106.

41. Mohan, R.R., Balne, P.K., Muayad, M.S., Tripathi, R., Sinha, N.R., Gupta, S., An, J.A., Sinha, P.R., and Hesemann, N.P. (2021). Six-month *in vivo* safety profiling of topical ocular AAV5-decorin gene transfer. Transl. Vis. Sci. Technol. *10*, 5.

42. Chaudhary, K., Moore, H., Tandon, A., Gupta, S., Khanna, R., and Mohan, R.R. (2014). Nanotechnology and adeno-associated virus-based decorin gene therapy ameliorate peritoneal fibrosis. Am. J. Physiol. Ren. Physiol. *307*, F777–F782.

43. Gupta, S., Sinha, N.R., Martin, L.M., Keele, L.M., Sinha, P.R., Rodier, J.T., Landreneau, J.R., Hesemann, N.P., and Mohan, R.R. (2021). Long-term safety and tolerability of BMP7 and HGF gene overexpression in rabbit cornea. Transl. Vis. Sci. Technol. *10*, 6.

44. Lim, R.R., Tan, A., Liu, Y.C., Barathi, V.A., Mohan, R.R., Mehta, J.S., and Chaurasia, S.S. (2016). ITF2357 transactivates Id3 and regulates TGFβ/BMP7 signaling pathways to attenuate corneal fibrosis. Sci. Rep. *6*, 20841.

45. Mohan, R.R., Tandon, A., Sharma, A., Cowden, J.W., and Tovey, J.C.K. (2011). Significant inhibition of corneal scarring in vivo with tissue-selective, targeted AAV5 decorin gene therapy. Invest. Ophthalmol. Vis. Sci. *52*, 4833–4841.

46. Anumanthan, G., Gupta, S., Fink, M.K., Hesemann, N.P., Bowles, D.K., McDaniel, L.M., Muhammad, M., and Mohan, R.R. (2018). KCa3.1 ion channel: a novel therapeutic target for corneal fibrosis. PLoS One *13*, e0192145.

47. Sharma, A., Anumanthan, G., Reyes, M., Chen, H., Brubaker, J.W., Siddiqui, S., Gupta, S., Rieger, F.G., and Mohan, R.R. (2016). Epigenetic modification prevents excessive wound healing and scar formation after glaucoma filtration surgery. Invest. Ophthalmol. Vis. Sci. *57*, 3381–3389.

48. Saika, S., Ikeda, K., Yamanaka, O., Flanders, K.C., Ohnishi, Y., Nakajima, Y., Muragaki, Y., and Ooshima, A. (2006). Adenoviral gene transfer of BMP-7, Id2, or Id3 suppresses injury-induced epithelial-to-mesenchymal transition of lens epithelium in mice. Am. J. Physiol. Cell Physiol. *290*, C282–C289.

49. Mody, A.A., Wordinger, R.J., and Clark, A.F. (2017). Role of Id proteins in BMP4 inhibition of profibrotic effects of TGF-β2 in human TM cells. Invest. Ophthalmol. Vis. Sci. *58*, 849–859.

50. Mody, A.A., Millar, J.C., and Clark, A.F. (2021). ID1 and ID3 are negative regulators of TGFβ2-induced ocular hypertension and compromised aqueous humor outflow facility in mice. Invest. Ophthalmol. Vis. Sci. *62*, 3.

51. Ko, M., Ahn, J., Lee, C., Chung, H., Jeon, S.H., Chung, H.Y., and Seong, R.H. (2004). E2A/HEB and Id3 proteins control the sensitivity to glucocorticoid-induced apoptosis in thymocytes by regulating the SRG3 expression. J. Biol. Chem. *279*, 21916–21923.

52. Wang, L.H., and Baker, N.E. (2015). E proteins and ID proteins: helix-loop-helix partners in development and disease. Dev. Cell *35*, 269–280.

53. Gloury, R., Zotos, D., Zuidscherwoude, M., Masson, F., Liao, Y., Hasbold, J., Corcoran, L.M., Hodgkin, P.D., Belz, G.T., Shi, W., et al. (2016). Dynamic changes

in Id3 and E-protein activity orchestrate germinal center and plasma cell development. J. Exp. Med. *213*, 1095–1111.

54. Teo, Z., Chan, J.S.K., Chong, H.C., Sng, M.K., Choo, C.C., Phua, G.Z.M., Teo, D.J.R., Zhu, P., Choong, C., Wong, M.T.C., and Tan, N.S. (2017). Angiopoietin-like 4 induces a β-catenin-mediated upregulation of ID3 in fibroblasts to reduce scar collagen expression. Sci. Rep. *7*, 6303.

55. Ma, J., Sanchez-Duffhues, G., Goumans, M.J., and Ten-Dijke, P. (2020). TGF-β-Induced endothelial to mesenchymal transition in disease and tissue engineering. Front. Cell Dev. Biol. *8*, 260.

56. Chang, C., Zhao, Q., Gonzalez, J.P., Kim, J.H., Alzahrani, K., Del-Re, D., and Fraidenraich, D. (2017). Hematopoietic Id deletion triggers endomyocardial fibrotic and vascular defects in the adult heart. Sci. Rep. *7*, 3079.

57. Tripathi, R., Giuliano, E.A., Gafen, H.B., Gupta, S., Martin, L.M., Sinha, P.R., Rodier, J.T., Fink, M.K., Hesemann, N.P., Chaurasia, S.S., and Mohan, R.R. (2019). Is sex a biological variable in corneal wound healing? Exp. Eye Res. *187*, 107705.

58. Gupta, S., Fink, M.K., Martin, L.M., Sinha, P.R., Rodier, J.T., Sinha, N.R., Hesemann, N.P., Chaurasia, S.S., and Mohan, R.R. (2020). A rabbit model for evaluating ocular damage from acrolein toxicity *in vivo*. Ann. N. Y. Acad. Sci. *1480*, 233–245.

59. Gouveia, R.M., Lepert, G., Gupta, S., Mohan, R.R., Paterson, C., and Connon, C.J. (2019). Assessment of corneal substrate biomechanics and its effect on epithelial stem cell maintenance and differentiation. Nat. Commun. *10*, 1496.

60. Wilhelmus, K.R. (2001). The Draize eye test. Surv. Ophthalmol. *45*, 493–515.

61. Altmann, S., Emanuel, A., Toomey, M., McIntyre, K., Covert, J., Dubielzig, R.R., Leatherberry, G., Murphy, C.J., Kodihalli, S., and Brandt, C.R. (2010). A quantitative rabbit model of vaccinia keratitis. Invest. Ophthalmol. Vis. Sci. *51*, 4531–4540.

62. Gupta, S., Kamil, S., Sinha, P.R., Rodier, J.T., Chaurasia, S.S., and Mohan, R.R. (2021). Glutathione is a potential therapeutic target for acrolein toxicity in the cornea. Toxicol. Lett. *340*, 33–42.